Int. J. Electrochem. Sci., 15 **(2020)** 4722 – 4738, doi: 10.20964/2020.05.13

International Journal of
ELECTROCHEMICAL
SCIENCE
www.electrochemsci.org

Ethylene Glycol Bis(Propionitrile) Ether as an Additive for SEI Film Formation in Lithium-Ion Batteries

Wen Liu[1,2,3], *Yueli Shi*[1,2,3], *Quanchao Zhuang*[1,2,3*], *Yongli Cuiab*[2,3], *Zhicheng Ju*[1.2.3], *Yanhua Cui*[d]

[1] Li-ion Batteries Lab, School of Materials Science and Engineering, China University of Mining & Technology, Xuzhou 221116, China
[2] the Jiangsu Province Engineering Laboratory of High Efficient Energy Storage Technology and Equipments under grant no. [2017]975-18
[3] the Xuzhou City Key Laboratory of High Efficient Energy Storage Technology and Equipments under grant no. KH17078
[4] Institute of Electronic Engineering China Academy of Engineering Physics, Mianyang, 621000, P. R. China
E-mail: zwysyl@163.com, zhuangquanchao@126.com

Received: 30 September 2019 / *Accepted:* 20 December 2019 / *Published:* 10 April 2020

The effect of ethylene glycol bis(propionitrile) ether(DENE) as a novel electrolyte additive on the electrochemical performance of a graphite anode was studied in this paper. Fourier transform infrared spectroscopy(FTIR), charge/discharge tests, cyclic voltammetry(CV), X-ray photoelectron spectroscopy(XPS), scanning electron microscopy(SEM), and electrochemical impedance spectroscopy(EIS) were used to investigate the SEI film and the cycle performance of graphite anode. The initial charge capacities of the graphite electrode in the electrolytes without and with 1% DENE were 319 $mAhg^{-1}$ and 349 $mAhg^{-1}$, respectively. After 60 cycles, the charge capacities without and with 1% DENE were 315 $mAhg^{-1}$ and 350 $mAhg^{-1}$, respectively. and the capacity retention rates were 95.8% and 98.1%, respectively. DENE promoted the formation of a thin and uniform SEI layer and improved the stability of the electrode. The addition of DENE effectively improved the electrochemical performance of graphite anodes.

Keywords: lithium-ion batteries; additive; Ethylene glycol bis(propionitrile) ether; solid electrolyte interface (SEI) film

1. INTRODUCTION

Lithium-ion batteries have always been the best electrochemical energy storage devices and are universally used in our world[1-3]. Currently, graphite has been widely adopted as an anode material for commercial lithium ion batteries due to its low cost and environmental friendliness [4, 5]. Moreover,

choosing the right electrolyte additive is a simple low-cost way to enhance the performance of lithium-ion batteries.[6]. A good quality electrolyte has a major impact on the battery capacity and cycle performance[7, 8]. During the first charge and discharge of a lithium-ion battery, part of the electrolyte is reduced on the graphite electrode to form a passivation layer, which is called a solid electrolyte interface (SEI). SEI film-forming additives have been extensively studied for their potential to improve the performance of SEI films[9, 10]. The SEI film prevents further disintegration of the electrolyte and inhibits graphite from breaking under a large negative voltage[11-13]. Studies have shown that the stability and rate properties of carbon electrodes can be improved by the formation of dense and stable SEI films[14-16].

This work aims to study the effect of DENE electrolyte additives on the performance of lithium-ion batteries. DENE is inexpensive, non-toxic, lipophilic and soluble in common electrolytes. We found that DENE could enhance the stability of the SEI film. DENE could directly participate in the synthesis of SEI membranes, but no electrochemical reduction occurs. Standard electrochemical techniques such as Fourier transform infrared spectroscopy (FTIR), cyclic voltammetry (CV), charge/discharge test, scanning electron microscopy (SEM), X-ray photoelectron spectroscopy (XPS) and electrochemical impedance spectroscopy (EIS), were used to analyse the electrochemical procedure. The results showed that DENE promotes the formation of a uniform, dense, thin and smooth SEI film to raise the reversible capacity and cycle stability of the graphite electrode.

2. EXPERIMENTAL

A slurry of electrodes was prepared by mixing 90 wt% graphite carbon fibre (MCF) and 10 wt% polyvinylidene fluoride (PVDF, HSV900) in N-methyl-2-pyrrolidone (NMP, electronic grade, Aladdin, 99.9%). The slurry was coated on a clean copper foil current collector by a coater (KTQ-II), and then dried under vacuum at 120 °C for 12 hours. The dry electrode was flattened at room temperature to make it smooth and compact. The fabricated electrode sheet should not be too thick, in order to minimize the impact of lithium ion transport in the porous electrode on the electrochemical impedance test. The electrolyte used was 1 M $LiPF_6$-EC:EMC (3:7 v/v Dongguan Shanshan Co, Ltd.). The DENE additives were placed in a glove box, and then different volumes of additives (0.3%, 1%, 2% and 4%) were added into the electrolyte.

FTIR was applied to analyse the structure of DENE. The charge-discharge test and CV were conducted with CR2032-type coin cells. The effects of different proportions of DENE on the electrochemical performance of graphite electrodes were investigated by CV and charge-discharge tests. CV was measured at a potential range of 3.0-0.01 V (vs. Li/Li^+) at a scan rate of 0.2 mV s^{-1}. The cells after the cycling measurements were disassembled in a glove box with an Ar atmosphere. The cycled graphite electrodes were rinsed in dimethyl carbonate (PanaxEtec) and to remove any residual electrolyte.

The effect of DENE addition on the surface structure and SEI morphology were analysed by field-emission scanning electron microscopy (FESEM, Oxford Instrument). The chemical composition on the graphite surface after the cycling measurements was analysed by XPS (Thermo Scientific, USA).

EIS testing was performed in a glass bottle with three-electrodes and Li foils as the counter and reference electrode. EIS testing is commonly used to study the electrochemical reactions that occur at the electrode/electrolyte interface. The experimental EIS data were fit and analysed using Z-View software.

3. RESULTS AND DISCUSSION

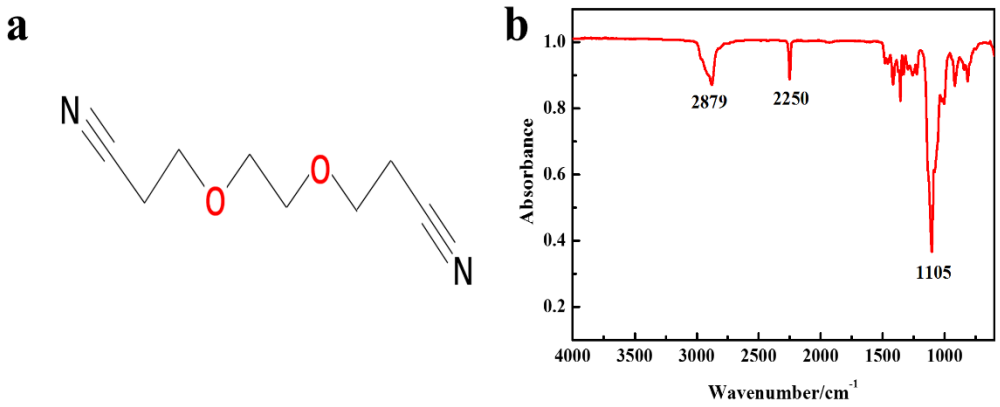

Figure 1. a Structures of the DENE; **b** FTIR spectra of the DENE

Fig 1a shows that the structure of DENE consists mainly of C≡N functional groups[17]. Fig.1b shows the infrared absorption spectra measured between 4000 cm^{-1} and 600 cm^{-1}. The peak at 2250 cm^{-1} was the tensile frequency of the nitrile triple bond, C≡N[18]. The peak corresponding to the stretching frequency of the C-O-C bond was observed at 1105 cm^{-1}. The peak corresponding to the stretching frequency of the C-H bond was observed at 2879 cm^{-1}.

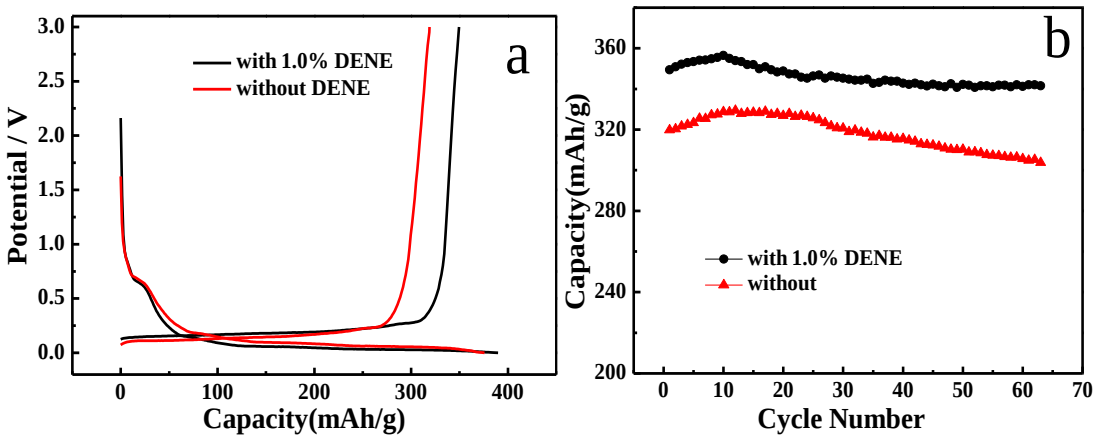

Figure 2. a The first charge-discharge characteristic of graphite electrode in electrolytes without and with 1% DENE **b** Cyclic charge performances of graphite electrode in electrolytes without and with 1% DENE

To determine the contribution of additive to the cycle performance, different proportions of DENE (0%, 0.3%, 1%, 2% and 4%) were added to the electrolyte. The cyclic charging performance of the graphite electrode in the electrolyte with different proportions of DENE is shown in Fig.S1 and Table S1. The electrode in the electrolyte containing 1% DENE showed the best cycle performance. This also indicated that DENE could only be used as an additive at an appropriate concentration.

Fig. 2 shows the cycle charge/discharge curves and cycle performance of the graphite electrodes in the electrolyte without and with 1% DENE. The curve in Fig. 2a shows that the charging capacity of the graphite electrode was improved after the addition of 1% DENE in the electrolyte, and the initial irreversible capacity decreased. In the electrolyte without DENE, the initial charge and discharge capacities were 319 $mAhg^{-1}$ and 375 $mAhg^{-1}$, respectively. After the addition of DENE in the electrolyte, the initial charge and discharge capacities of the graphite electrode were 349 $mAhg^{-1}$ and 389 $mAhg^{-1}$, respectively. Then, the capacity value gradually stabilized. It could be concluded that the charge and discharge capacity of the graphite electrode was improved after the addition of the electrolyte containing DENE. The coulombic efficiencies were 84.9% and 89.6% for the electrolytes without and with DENE, respectively. The addition of DENE in the electrolyte significantly reduced the irreversible capacity and increased the coulombic efficiency of the graphite electrode.

Fig. 2b shows the cycle performance and efficiency of the graphite electrode without and with 1% DENE. The initial charge capacities of the graphite electrode were 319 $mAhg^{-1}$ and 349 $mAhg^{-1}$, respectively. The charge capacity of the graphite electrode gradually increased with the number of charge-discharge cycles in the first 10 weeks. After 10 weeks, the capacity was 329 $mAhg^{-1}$ and 356 $mAhg^{-1}$, respectively, and the capacity gradually stabilized. The graphite electrode had a charge capacity of 305 $mAhg^{-1}$ and 341 $mAhg^{-1}$ after 60 cycles and a capacity retention of 95.6% and 97.7%, respectively, compared to the first cycles. It was clear from the figure that the graphite electrode in the electrolyte with DENE had better capacity retention and cycle stability. Since a battery with 1% DENE provided optimum cycle performance, the effect of 1% DENE on the graphite electrode was investigated using electrochemical and chemical characterization techniques as described below.

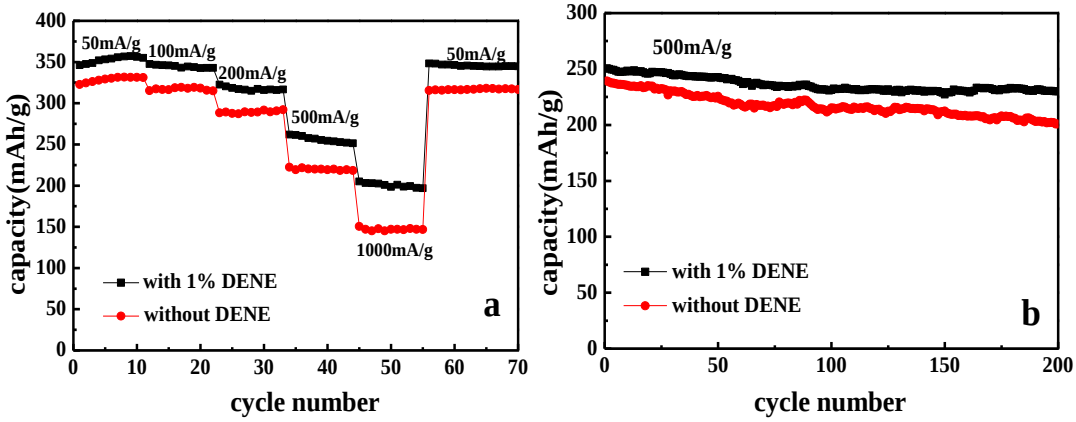

Figure 3. Rate capability performances (**a**) and high rate performances (**b**) of graphite electrodes without and with 1% DENE

The rate capabilities of graphite electrodes in the electrolyte without and with 1% DENE were evaluated at various discharge-charge rates. Fig. 3a shows the cycle performance of the graphite

electrode in the electrolyte without and with 1% DENE at various discharge-charge rates. The reversible capacity of the graphite electrode without DENE was 322, 315, 288, 222 and 150 $mAhg^{-1}$ at current densities of 50, 100, 200, 500 and 1000 mAg^{-1}, respectively. In contrast, the graphite electrode in the electrolyte with 1% DENE provided much higher reversible capacities of 346, 347, 322, 261 and 204 $mAhg^{-1}$, respectively. This demonstrated a superior variable-rate performance for the graphite electrodes in the electrolyte with 1% DENE.

Fig. 3b shows the cycle curve of the graphite electrode in an electrolyte with and without 1% DENE at a current density of 500 mAg^{-1}. The capacity of the latter was higher than the capacity of the former. The corresponding first cycle capacities were 239 $mAhg^{-1}$ and 250 $mAhg^{-1}$, respectively. The corresponding capacities were 200 $mAhg^{-1}$ and 229 $mAhg^{-1}$ after 200 cycles, and the capacity retention rates were 83.7% and 91.6%, respectively. This demonstrates the excellent performance of graphite electrodes in electrolytes with 1% DENE at a current density of 500 $mAhg^{-1}$.

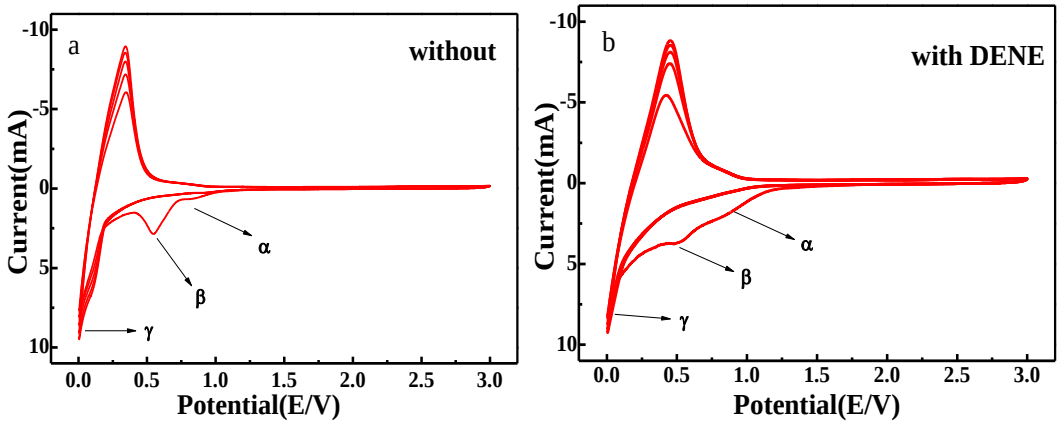

Figure 4. The CV curves of graphite electrode in different electrolytes: **a** without additives; **b** with 1% DENE

The CV curve results of the electrode, as shown in Fig. 4, were obtained in the electrolyte without and with DENE additive[19]. Fig. 4a shows the CV cycle curve of a graphite electrode without additives in the electrolyte. Fig. 4a shows three current peaks (reduction peak α, reduction peak β and reduction peak γ) in the graphite electrode during the first scan from open circuit potential to low potential[20]. The peak α corresponded to the reduction of EC to Li_2CO_3 at 0.8 V (single electron reduction process), the peak β at 0.5 V, was consistent with the reduction of EC to lithium alkylate (double-electron reduction process)[21, 22], and the peak γ at 0 V confirmed that the lithium ion was embedded into the graphite electrode.

In the electrolyte with 1% DENE, the peaks were similar to those of the cyclic voltammetry curve in the electrolyte without additives. The peak value γ of the characteristic peak near 0.02 V remains the same. Meanwhile, the peaks α and β associated with the EC reduction process were slightly smoothed. It was shown that the electrolyte with 1% DENE could better inhibit the decomposition of EC[23].

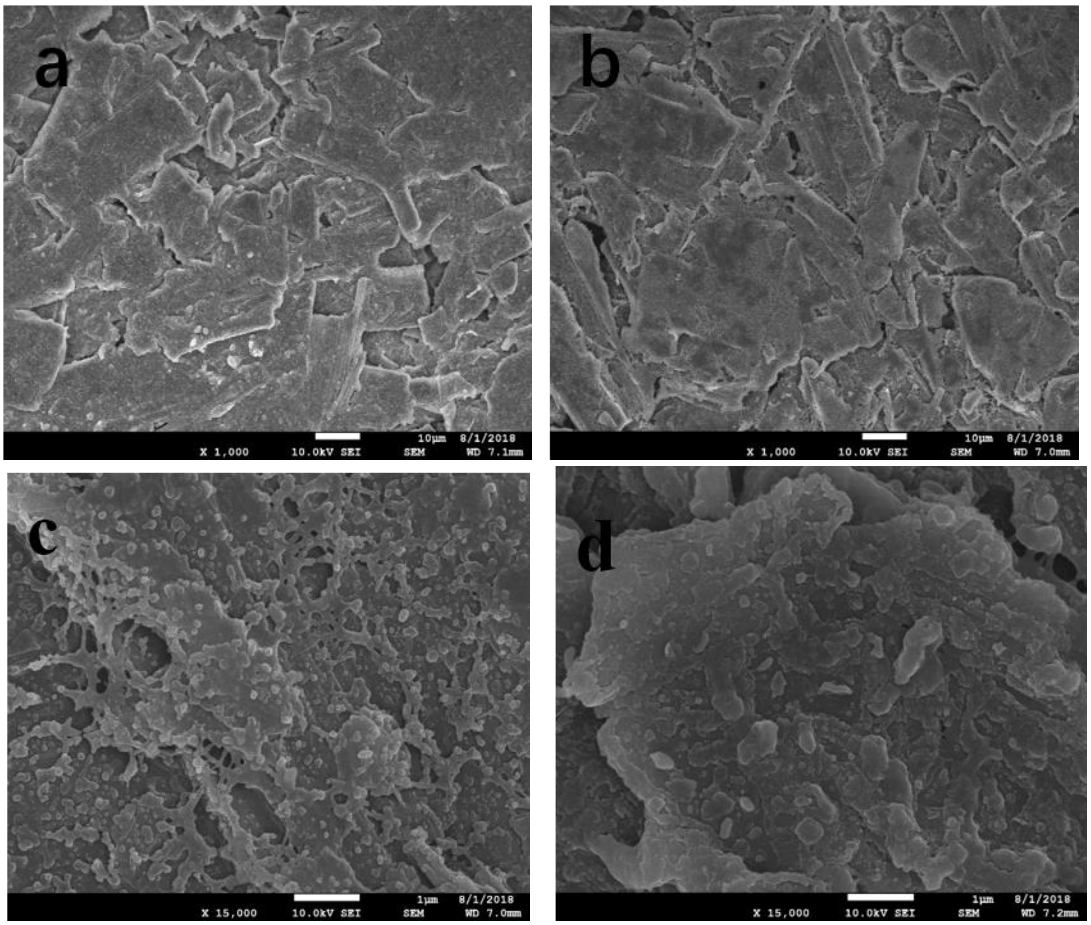

Figure 5. SEM images of graphite electrode after CV cycle in the electrolyte without DENE (a),(c) and with 1% DENE (b),(d)

Fig. 5 shows SEM images of the graphite electrode after cycling in the electrolytes with and without DENE. In the electrolyte without DENE (Fig.5a and c), there were some small grain sizes on the graphite electrode surface. The SEM image of the surface of the graphite electrode in the electrolyte containing DENE showed a smooth and dense morphology, as shown in Fig.5b and d. Hence, DENE promoted the formation of a dense and smooth SEI film that was beneficial for an enhanced cycle performance. This alleviated the undesirable osmotic side reaction between the electrolyte and the negative graphite electrode[24].

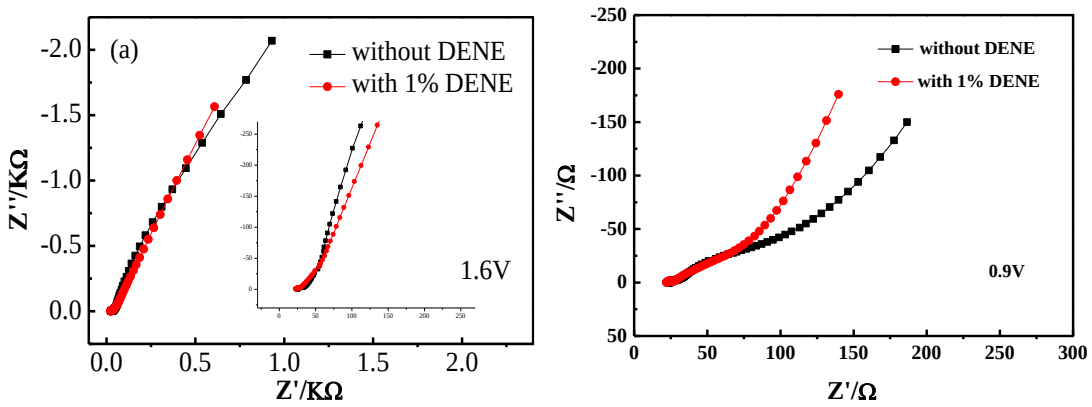

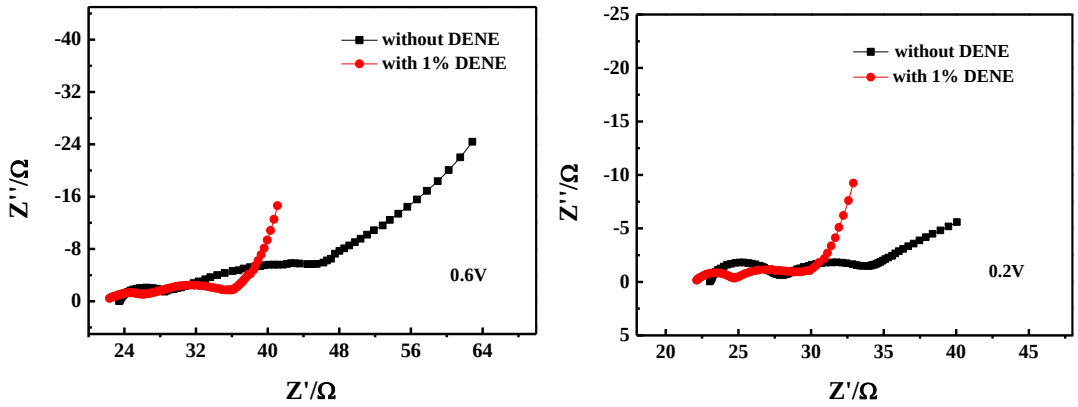

Figure 6. Nyquist diagrams of the graphite electrode in the first discharge process without and with 1% DENE at various potentials: **a** 1.6V, **b** 0.9V, **c** 0.6V and **d** 0.2V

To explore the modification mechanism of additive DENE on the surface of the graphite electrode, EIS testing was applied[22, 25]. Fig. 6 and Fig. S2–S7 showed the electrochemical impedance spectroscopy of the first discharge of graphite electrodes without DENE and with 1% DENE. When the potential was greater than 0.9 V, the EIS of the graphite electrode showed that the high frequency region was a semicircle (HFS), and the low frequency region was a line (LFL)[26, 27]. The results showed that the surface of the graphite electrode did not decompose to form an SEI film before the potential was 0.9 V. When the electrode potential was polarized to 0.7 V, it could be clearly seen from the EIS spectrum that the line and curve in the LFL formed a semicircle and a slanted line. Furthermore, the EIS was composed of an HFS and a semicircle generated by an intermediate frequency region (MFS) and LFL. According to Aurbach et al.'s study, an HFS in the high frequency region was related to the process of reductive decomposition of the SEI film formed on the graphite electrode by the electrolyte. MFS was associated with the charge transfer of the graphite electrode to the electrolyte in the lithium cell. LFL reflected the solid diffusion of lithium ions in the graphite of the electrode[28-31]. The above results were completely consistent with their inference results. Fig.S8 showed a comparison of the EIS data and the fitted results at 0.6 V. Table S2 reveals the equivalent circuit parameters of Nyquist fitting results in the first discharge cycle at 0.6 V in the electrolyte without and with 1% DENE. Table S2 shows that the fitting results agree well with the experimental data, and the errors of R_{SEI} and Rct were less than 10%.

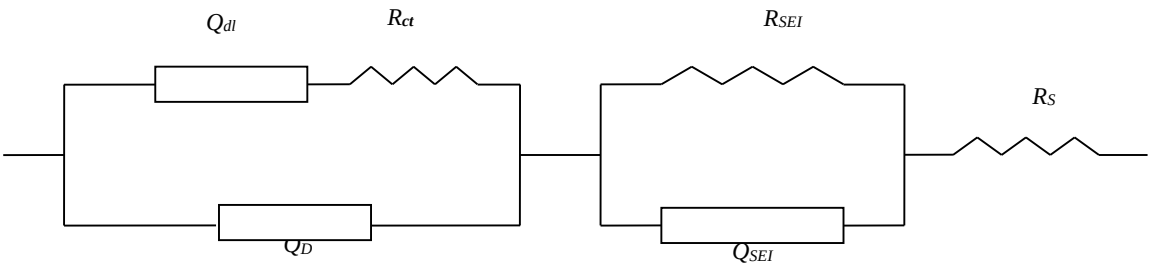

Figure 7. Equivalent circuit proposed for fitting impedance spectra

The equivalent circuit, as shown in Fig. 7, explained the principle of the impedance spectrum[32]. In the equivalent circuit, the resistor-capacitor circuit (RC) marks the semicircle in the Nyquist plot. The constant phase angle element CPE(Q) represents a capacitor. R_S and R_{SEI} represent the resistance of the surface and the SEI film, respectively. Q_{SEI} represents the capacitance of the contact resistance. The resistance of the charge transfer in the intermediate frequency region and the capacitance of the double layer are represented by R_{ct} and Q_{dl}. The impedance associated with the diffusion in the low frequency region is represented by Q_D[33-35]. The equivalent circuit diagram could effectively characterize the interface reaction of the graphite electrode to better fit the experimental data. A CPE is an element used to characterize the non-ideal behaviour of an electrode. The formula for CPE is as follows:

$$Y = Y_0 w^n \cos\left(\frac{n\pi}{2}\right) + jY_0 w^n \sin\left(\frac{n\pi}{2}\right)$$

In the above formula, ω represents the angular frequency. The elements represented by the CPE vary with the value of n. The CPE is a capacitor when the value of n is 1. The CPE is a purely resistive element when n = 0, and when n = -1, the CPE is an inductive element. The CPE is a Warburg impedance when n = 0.5.

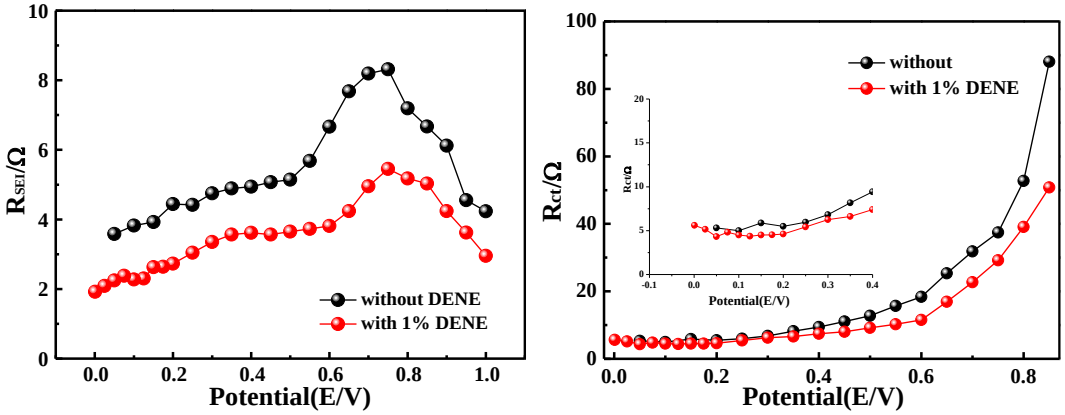

Figure 8a The values of R_{SEI} at different electrode potentials in the electrolyte without and with 1% DENE , **b** The values of R_{ct} at different electrode potentials in the electrolyte without and with 1% DENE

Fig. 8a shows the variation of R_{SEI} for a graphite electrode obtained in the electrolytes with and without DENE. The formula is, $R_{SEI}L = \rho/(S)$, where L, ρ, and S represent the thickness, resistivity, and surface area of the SEI film, respectively. The surface area of the graphite electrode is constant. Therefore, the change in resistance R_{SEI} reflects the thickness of the SEI film[36]. When the electrode potential dropped to 0.7 V, the value of R_{SEI} rapidly increased as the electrode potential decreased. At this point, the SEI film formed and gradually thickened. When the electrode potential decreased from 0.75 V to 0.35 V, the SEI resistance rapidly decreased. This process may be related to the reductive decomposition of EC solvent molecules in the electrolyte[37]. The R_{SEI} of the graphite electrode after the addition of the DENE additive was similar to that of the above trend. It could be seen from the fitting diagram that the R_{SEI} resistance value of the graphite electrode after adding the DENE additive in the electrolyte was obviously lower than that of the R_{SEI} resistance value of the electrolyte without additives, which corresponded to the CV test result. This showed that the R_{SEI} resistance of the graphite electrode

after the addition of the DENE additive in the electrolyte was obviously lower than the R_{SEI} resistance without additives in the electrolyte, which proved that adding the DENE additive could form a thinner SEI film on the interface of graphite electrode to improve the electrochemical performance of lithium ion battery.

Fig. 8b shows the graph of R_{ct} versus electrode potential during graphite electrode polarization from the open circuit potential to a low potential. It can be seen from Fig.6b that the same trend of R_{ct} in all electrolyte systems decreases with the decrease of the graphite electrode from the open circuit potential to the lowest potential. The R_{ct} of the graphite electrode after adding the DENE additive in the electrolyte was obviously smaller than the R_{ct} of the graphite electrode after not adding the additive. The value of R_{ct} indicated the difficulty of the charge-transfer process of the battery. This showed that the addition of the DENE additive in the electrolyte facilitated the insertion/extraction of lithium ions in the graphite electrode.

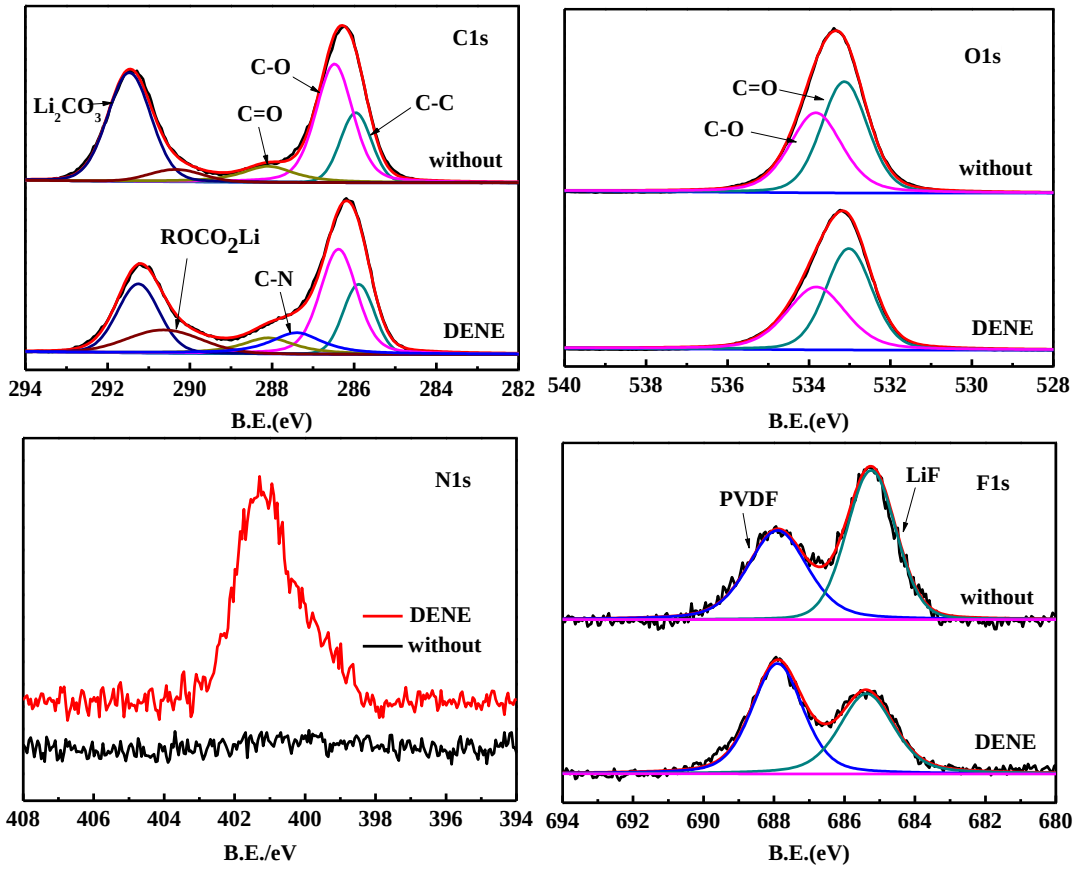

Figure 9. XPS spectra of graphite electrode after 70 cycles without and with 1% DENE:**a** C 1s, b O 1s, c N 1s and d F 1s

Fig. 9 shows the XPS spectra of the graphite electrode after cycling in the electrolytes with and without DENE. In the C1 s spectra (Fig. 9a), the peaks at 291.5 eV, 290.5 eV, 288 eV, 286.5 eV and 285.8 eV, corresponded to Li_2CO_3, lithium alkyl carbonate($ROCO_2$ Li), C=O, C-O, C-C, respectively[38]. Li_2CO_3 and $ROCO_2$ Li were the main components of the SEI film[39]. The SEI film containing lithium carbonate alkyl ester ($ROCO_2$ Li) was beneficial to the electrochemical performance

of lithium-ion batteries[40]. In the C1 s spectrum with the DENE additive, the presence of C-N indicated that DENE was involved in the reaction[18]. However, the peak intensity representing the electrolyte decomposition product Li_2CO_3 was much stronger for the electrode in the blank electrolyte than that of the electrode in the DENE electrolyte, indicating that the addition of DENE reduced the formation of Li_2CO_3. The O1 s spectra (Fig. 9b) with and without DENE were basically similar. In the N1 s spectra (Fig. 9c), N could be detected on the graphite electrode circulating in the electrolyte containing DENE, but N could not be detected in the electrolyte without DENE, confirming that the decomposition product of DENE had been incorporated into the SEI film[41]. In the F1 s spectra (Fig. 9d), the peaks at 687.9 eV and 685.5 eV corresponded with PVDF and LiF[41, 42]. The intensity of the LiF peak of the electrode in the electrolyte without DENE was much stronger than that of the electrode with the DENE electrolyte. This difference indicated that DENE could suppress the decomposition of the electrolyte circulating on the graphite electrode. The DENE additive was involved in the reaction and improved the composition of the SEI film, which was advantageous for the electrochemical performance of the graphite electrode.

4. CONCLUSIONS

The effects of DENE on graphite anodes were investigated by electrochemical performance tests, SEM, XPS and FTIR. As a novel stable electrolyte additive, DENE reacted with electrochemically reduced radical anions in the EC to form a SEI. The initial charge capacity and the capacity retention ratio of the graphite electrode in the electrolyte with DENE were improved. After 60 cycles, the capacity retention rates in the electrolytes with and without DENE were 95.8% and 98.1%, respectively. DENE reduced the variation of R_{SEI}, facilitated the formation of a thin and uniform SEI film and improved its stability on the negative graphite electrode. Therefore, the electrochemical performance such as the cycle stability and the reversible capacity of the graphite electrode, was improved.

CONFLICTS OF INTEREST
There are no conflicts to declare.

ACKNOWLEDGMENTS
This work was supported by the Fundamental Research Funds for the China University of Mining and Technology(2017XKQY063)

SUPPLEMENTARY INFORMATION

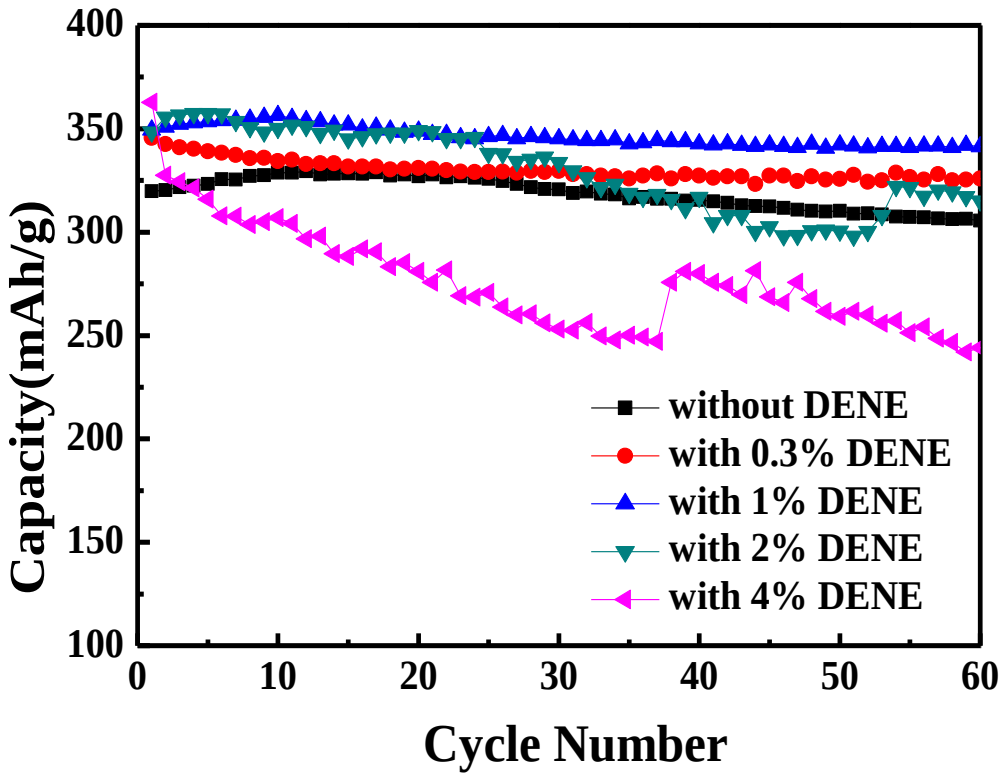

Figure S1 Cyclic charge performance of graphite electrode with different composition of electrolytes

Table S1 Cyclic charge performance of graphite electrode with different of electrolytes

	Without DENE	0.3% DENE (saturation)	1% DENE	2% DENE	4% DENE
Initial charge specific capacity (mAh g^{-1})	319.77	345.67	349.39	348.38	362.71
After 60cycles	305.65	326	341.54	315.08	244.12
Capacity retention (%)	95.6	94.3	97.75	90.4	67.3

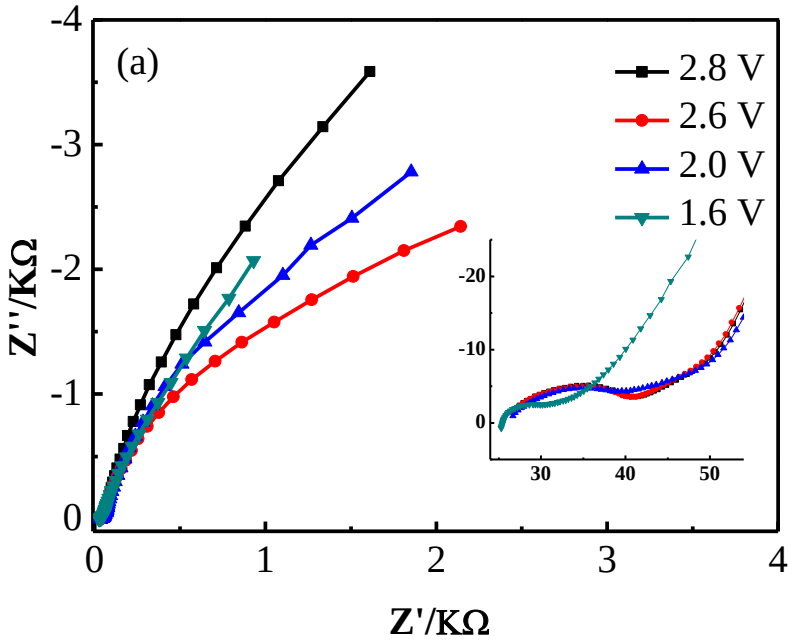

Figure S2 The Nyquist diagrams of the graphite electrolyte at various potentials from 2.8 to 1.6V in the first discharge process in the electrolyte without DENE

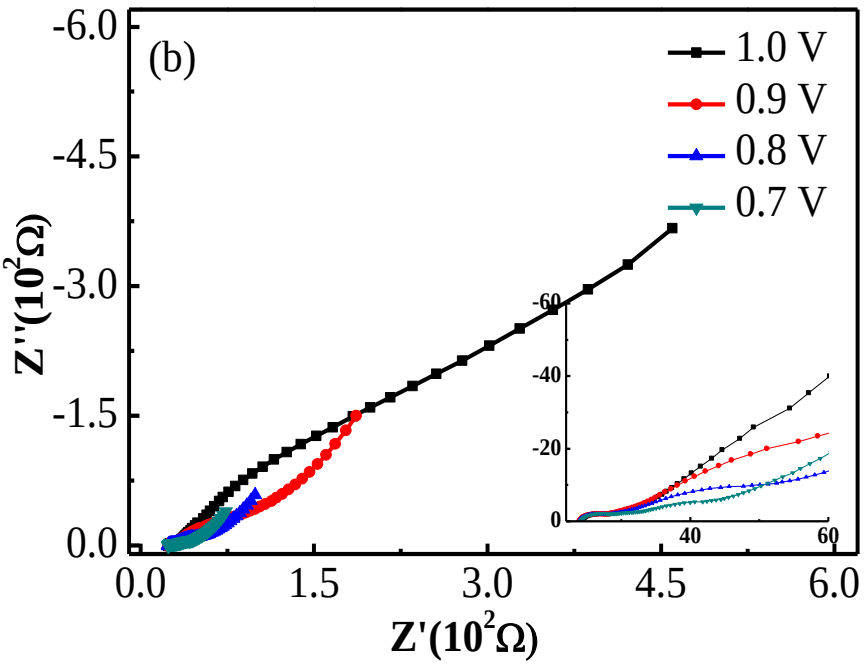

Figure S3 The Nyquist diagrams of the graphite electrolyte at various potentials from 1.0to 0.7V in the first discharge process in the electrolyte without DENE

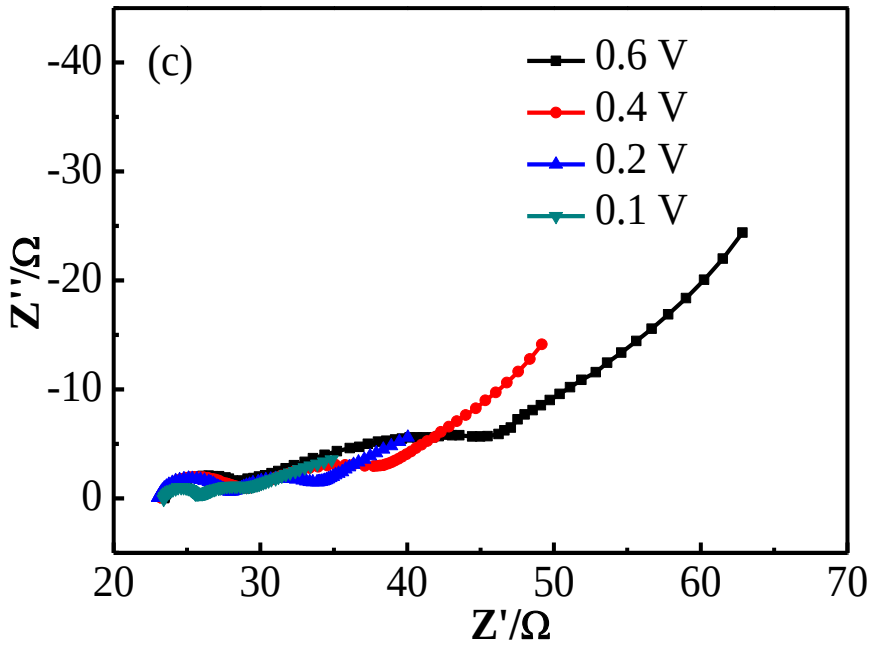

Figure S4 The Nyquist diagrams of the graphite electrolyte at various potentials from 0.6 to 0.1V in the first discharge process in the electrolyte without DENE

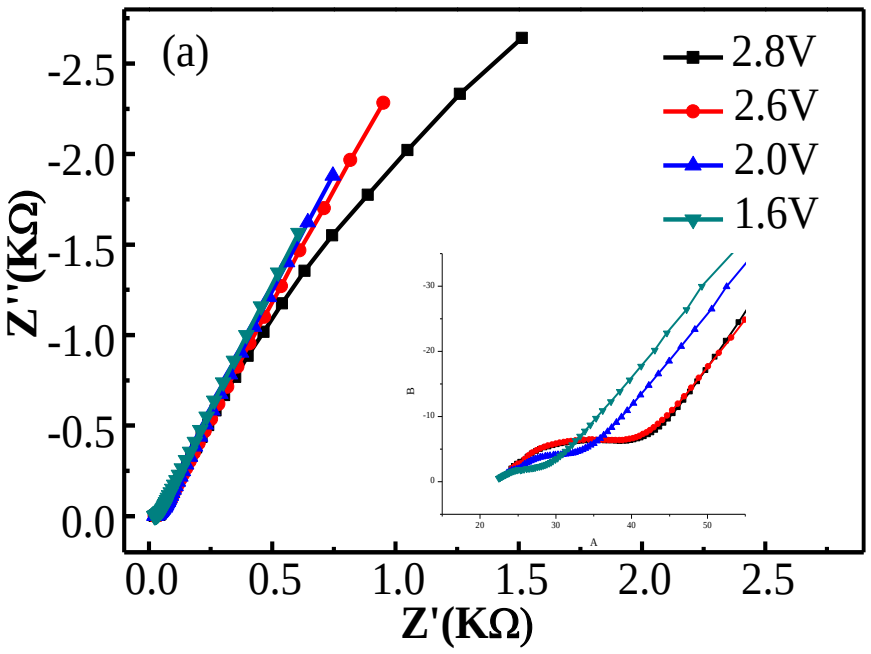

Figure S5 The Nyquist diagrams of the graphite electrolyte at various potentials from 2.8 to 1.6V in the first discharge process in the electrolyte with 1% DENE

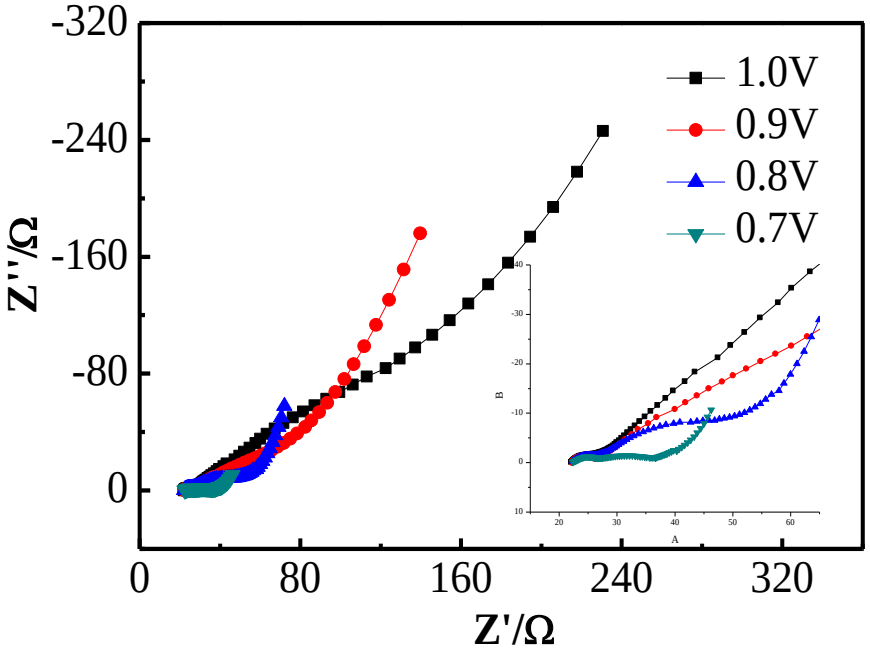

Figure S6 The Nyquist diagrams of the graphite electrolyte at various potentials from 1.0 to 0.7V in the first discharge process in the electrolyte with 1% DENE

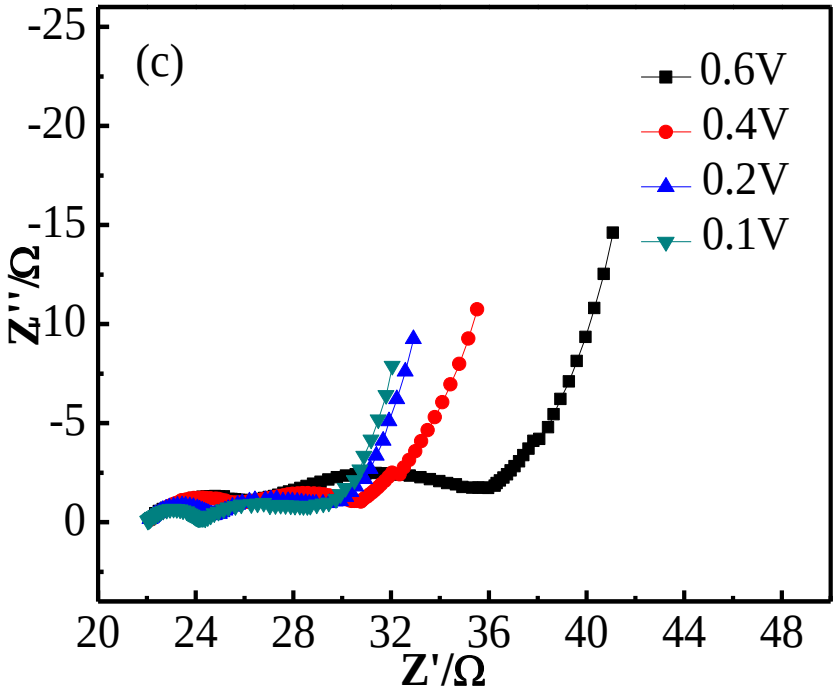

Figure S7 The Nyquist diagrams of the graphite electrolyte at various potentials from 0.6 to 0.1V in the first discharge process in the electrolyte with 1% DENE

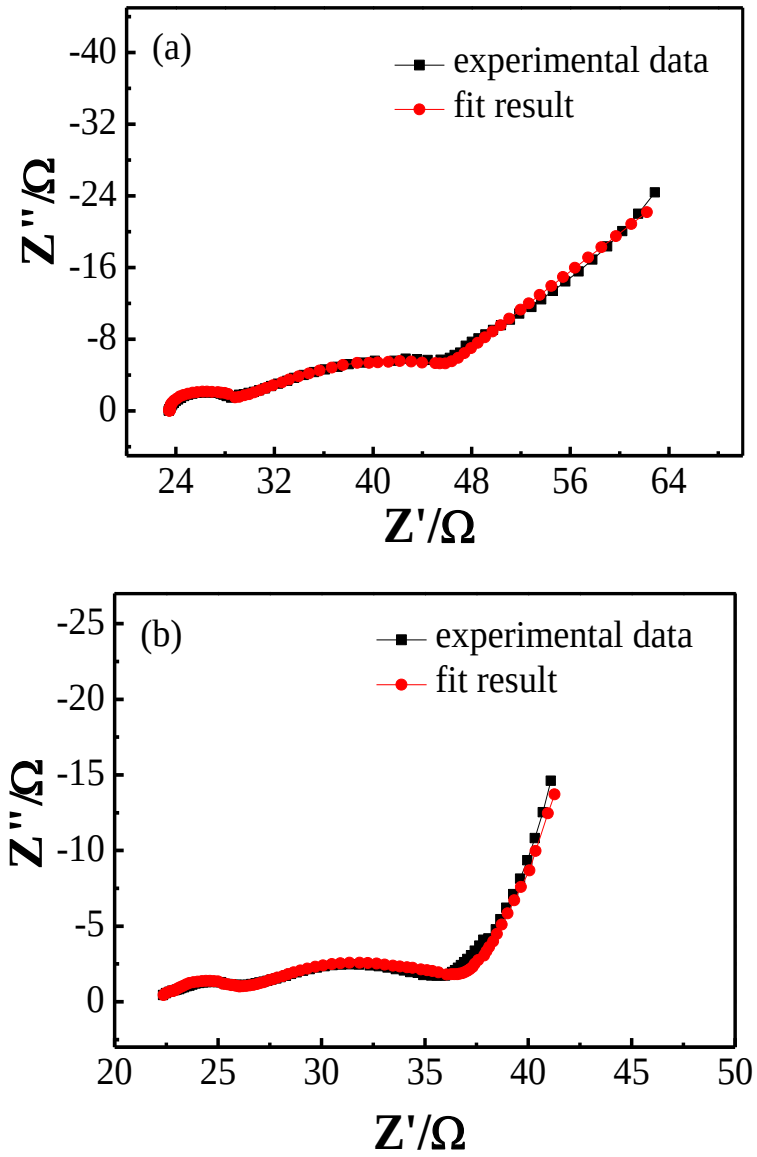

Figure S8 Comparison of EIS data and fit result at 0.6V (**a**): Without DENE and (**b**): With 1% DENE

Table S2 Equivalent circuit parameters of Nyquist fitting results in the first discharge cycle at 0.6V in the electrolyte without and with 1% DENE

Element	In the electrolyte without DENE		In the electrolyte with 1% DENE	
	Value	Error%	Value	Error%
R_S	23.47	0.576	22.14	1.074
R_{SEI}	6.67	4.586	3.82	6.547
Q_{SEI}-n	0.68	7.193	0.657	11.187
Q_{SEI}-Y_0	6.49E-4	19.699	8.14E-4	24.046
Rct	18.35	6.1672	11.54	9.417
Q_{dl}-n	0.794	4.7072	0.8524	6.1505
Q_{dl}-Y_0	0.005853	8.8031	0.00268	14.268
Q_D-n	0.64	4.641	0.45	7.561
Q_D-Y_0	1.52	2.452	1.06	3.684

References

1 H. Su, A.A. Barragan, L. Geng, D. Long, L. Ling, K.N. Bozhilov, L. Mangolini, J. Guo, *Angew. Chem. Int. Ed.*, 56 (2017) 10780.
2 Z. Liu, L. Feng, X. Su, C. Qin, K. Zhao, F. Hu, M. Zhou, Y. Xia, *J. Power Sources*, 375 (2018) 102.
3 Y. An, H. Fei, G. Zeng, L. Ci, S. Xiong, J. Feng, Y. Qian, *Acs Nano* 12(2018)4993.
4 B. Moradi, G.G. Botte, *J. Appl. Electrochem.*, 46 (2016) 123.
5 A. Balducci, A. Brandt, P. Isken, A. Lexbalducci, *J. Power Sources*, 204 (2012) 213.
6 T. Yim, Y.K. Han, *ACS Appl. Mater. Interfaces*, 9 (2017)32851.
7 M. Zhao, X. Zuo, X. Ma, X. Xiao, L. Yu, J. Nan, *J. Power Sources*, 323 (2016) 29.
8 R. Wagner, S. Brox, J. Kasnatscheew, M. Amereller, I. Cekic-Laskovic, M. Winter, *Electrochem. Commun.*, 40 (2014) 80.
9 A.M. Colclasure, K.A. Smith, R.J. Kee, *Electrochim. Acta*, 58 (2011) 33.
10 Y. Zhu, I.A. Shkrob, D.P. Abraham, *J. Electrochem. Soc.* 30 (2014) 11.
11 F. Dinkelacker, P. Marzak, J. Yun, Y. Liang, A.S. Bandarenka, *ACS Appl. Mater. Interfaces*, 10 (2018) 14063.
12 J. Xia, L. Madec, L. Ma, L.D. Ellis, W. Qiu, K.J. Nelson, Z. Lu, J.R. Dahn, *J. Power Sources*, 295 (2015) 203.
13 K.C. Möller, H.J. Santner, W. Kern, S. Yamaguchi, J.O. Besenhard, M. Winter, *J. Power Sources*, 119 (2003) 561.
14 J. Xia, L. Madec, L. Ma, L.D. Ellis, W. Qiu, K.J. Nelson, Z. Lu and J.R. Dahn, *J. Power Sources.*, 295 (2015) 203.
15 M.T.F. Rodrigues, F.N. Sayed, H. Gullapalli, P.M. Ajayan, *J. Power Sources*, 381 (2018) 107.
16 F. Chrétien, J. Jones, C. Damas, D. Lemordant, P. Willmann, M. Anouti, *J. Power Sources*, 248 (2014) 969.
17 R. J. Chen, F. Liu, Y. Chen, Y. S. Ye, Y. X. Huang, F. Wu, L. Li, *J. Power Sources*, 306 (2015) 70.
18 H. Duncan, N. Salem, Y. Abu-Lebdeh, *J. Electrochem. Soc*., 160 (2013) A838.
19 P.T. Kissinger, W.R. Heineman, *J. Chem. Educ.*, 60 (1983) 702.
20 A.M. Haregewoin, E.G. Leggesse, J.C. Jiang, F.M. Wang, B.J. Hwang, S.D. Lin, *Electrochim. Acta*, 136 (2014) 274.
21 A. Naji, J. Ghanbaja, B. Humbert, P. Willmann, D. Billaud, *J. Power Sources*, 63 (1996) 33.
22 O. Chusid, E.E. Ely, D. Aurbach, M. Babai, Y. Carmeli, *J. Power Sources*, 43 (1993) 47.
23 D. Aurbach, K. Gamolsky, B. Markovsky, Y. Gofer, M. Schmidt, U. Heider, *Electrochim. Acta*, 47 (2003) 1423.
24 D. Farhat, J. Maibach, H. Eriksson, K. Edstrom, D. Lemordant, F. Ghamouss, *Electrochim. Acta*, 281 (2018) 299.
25 S.D. Xu, Q.C. Zhuang, L.L. Tian, Y.P. Qin, L. Fang, S.G. Sun, *J. Phys. Chem.* C, 115 (2011) 9210.
26 X.Y. Qiu, Q.C. Zhuang, Q.Q. Zhang, R. Cao, Y.H. Qiang, P.Z. Ying, S.G. Sun, *J. Electroanal. Chem.*, 687 (2012)35.
27 L.I. Ge-Chen, G.U. Yan-Lei, Chinese *J. Power Sources* 32(2008)119.
28 M.D.L. And, D. Aurbach, *J. Phys. Chem.* B, 101 (1997) 4630.
29 D. Andre, M. Meiler, K. Steiner, C. Wimmer, T. Soczka-Guth, D.U. Sauer, *J. Power Sources*, 196 (2011) 5334.
30 X.Y. Qiu, Q.C. Zhuang, Q.Q. Zhang, R. Cao, Y.H. Qiang, P.Z. Ying, S.G. Sun, *J. Electroanal. Chem.*, 687 (2012) 35.
31 D. Aurbach, M.D. Levi, E. Levi, A. Schechter, *J. Phys. Chem*. B, 101 (1997) 2195.
32 L. Li, F. Wu, R.J. Chen, S.X. Wu, *Chemical Journal of Chinese Universities*, 28 (2007) 293.

33 X. Zhao, Q.C. Zhuang, Y.L. Shi, X.X. Zhang, *J. Appl. Electrochem*., 45 (2015) 1013.
34 J. Guo, A. Sun, X. Chen, C. Wang, A. Manivannan, *Electrochim. Acta*, 56 (2011) 3981.
35 M. Itagaki, N. Kobari, S. Yotsuda, K. Watanabe, S. Kinoshita, M. Ue, *J. Power Sources*, 135 (2004) 255.
36 Q.-C. Zhuang, J. Li, L.-L. Tian, *J. Power Sources*, 222 (2013) 177.
37 C. Wang, A.J. Appleby, F.E. Little, *J. Electroanal. Chem*. 497 (2001) 33.
38 L. Chen, K. Wang, X. Xie, J. Xie, *J. Power Sources*, 174 (2007) 538.
39 P. Verma, P. Maire, P. Novák, *Electrochim. Acta*, 55 (2010) 6332.
40 S.J. An, J.L. Li, C. Daniel, D. Mohanty, S. Nagpure, D.L. Wood, *Carbon*, 105 (2016) 52.
41 X. Wang, X. Zheng, Y. Liao, Q. Huang, L. Xing, M. Xu, W. Li, *J. Power Sources*, 338 (2017) 108.
42 K. Wang, L. Xing, H. Zhi, Y. Cai, Z. Yan, D. Cai, H. Zhou, W. Li, *Electrochim. Acta*, 262 (2018) 226.